Journal of Nuclear Materials 266–269 (1999) 1230–1233

A fast scanning Langmuir probe system for ASDEX-Upgrade divertor

N. Tsois [a,*], C. Dorn [b], G. Kyriakakis [a], M. Markoulaki [a], M. Pflug [b], G. Schramm [b], P. Theodoropoulos [a], P. Xantopoulos [a], M. Weinlich [b], the ASDEX Upgrade Team[b]

[a] *NCSR 'Demokritos', Inst. of Nucl. Technol-Rad. Prot., 153 10 Ag. Paraskevi-Attiki, Athens, Greece*

[b] *Max-Planck-Institut für Plasmaphysik, EURATOM Association, Garching, Germany*

Abstract

A fast scanning Langmuir probe system (LPS) for ASDEX-Upgrade's divertor plasma investigations was designed, manufactured and operated. Profiles of ion saturation current density, J_{sat}, electron temperature, T_{ed}, electron density, N_{ed}, floating potential, V_{fl}, and Mach number have been recorded for ohmic (OH) and low/medium power neutral beam heated (NI) discharges. In these cases the probe can access both divertor legs, allowing comparison of plasma parameters in the two divertors and investigations of the private flux region. Strong divertor asymmetries, complex plasma flow patterns and changes in the power flow to the divertor targets, depending on ion grad**B** drift direction, density and divertor geometry, have been observed.

Keywords: ASDEX-Upgrade; Langmuir probe; Divertor plasma; Plasma flow

1. Introduction

Divertors are presently the main option for solving a number of critical and often conflicting design requirements for a fusion reactor based on magnetic confinement. Detailed investigations of the plasma parameters and of the ion dynamics in the divertor area in conjunction with their modelling represent very important tasks in magnetic fusion research. Due to their characteristics (spatial and temporal resolution, direct relevance for plasma – materials interactions etc.) Langmuir probes can fruitfully contribute to this effort and are used in all presently operated tokamaks [1–3] despite some still open interpretation problems [4]. In this paper we present the first results obtained with a fast scanning Langmuir probe system (LPS) designed, manufactured and operated in ASDEX-Upgrade divertor area by the team of Plasma Physics Laboratory of NCSR 'Demokritos' in the framework of the Max-Planck-Institut für Plasmaphysik (IPP) – NCSR 'Demokritos' co-operation and under an EURATOM contract [5].

2. Apparatus

The LPS is a fully computer controlled manipulator system, 7 m long at full extension, capable to 'fast scan' in radial and poloidal directions the plasma in the AUG's divertor area (Fig. 1). In order to minimise the inertial forces, the front part of the LPS has been splitted in three blocks: the *positioning block*, the *fast moving block*, and the *probe arm*. (Fig. 1(a)). In this way the really fast moving part (the *probe arm*) weighs only a few hundred grams.

A full stroke of 40 cm, a tilting angle to the horizontal plane of 30°, a speed of 3 m/s and an acceleration of 3 g are the limits of the system. Using only electrical actuators (servo and step motors) an arbitrary 'wave form' of the movement can be pre-programmed within these limits. Up to six electrodes can be biased in an arbitrary arrangement (single, double, triple, floating or

* Corresponding author. Tel.: +30 1 650 3802; fax: +30 1 653 3431; e-mail: nit@ipta.demokritos.gr/nit@ipp.mpg.de

0022-3115/99/$ – see front matter
PII: S0022-3115(98)00569-8

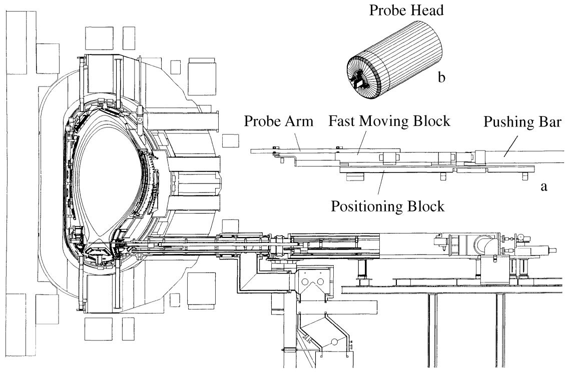

Fig. 1. General layout of LPS in ASDEX-Upgrade's octant cross section. (a) The front part of the system, (b) Mach probe head arrangement.

grounded) using a computer controlled relay board. 'Mach' probe heads made of CFC have been mainly used (Fig. 1(b)). 8 Mb of data per shot, at sampling rates up to 1 MHz, are routinely recorded. A detailed description of the LPS can be found in [6].

3. Experimental results

The LPS has been operated in the last experimental phase of DIV-I configuration of AUG in 1996 and, after some modifications imposed by the new, narrow, access slit, in the new DIV-II configuration. We present here some of the results obtained during these phases of operation.

*3.1. DIV-I Profiles. Influence of ion grad**B** drift direction*

The influence of ion grad**B** drift direction on divertor parameters (electron temperature T_{ed}, density N_{ed} and floating potential V_{fl}, in both divertor legs) have been observed in DIV-I, OH shots (Fig. 2) (plasma current $I_p = \pm(600 - 800)$ kA, toroidal field $B_t = \pm 2.1$ T, line averaged density $\langle N_e \rangle = 2\text{–}4 \times 10^{19}$ m^{-3}, power to the scrape off layer $P_{SOL} = 300\text{–}400$ kW). In the AUG's 'normal polarity' (ion grad**B** towards the X point), the inner divertor is colder $T_{ed\_in}/T_{ed\_out} \leqslant 1/2$) and denser $N_{ed\_in}/N_{ed\_out} \approx 2$) while the two divertors are approximately symmetric in the 'reverse polarity' (ion grad**B** away from the X point). In the accuracy of Langmuir probe measurements, pressure balance exists between mid plane and the two divertors $P_{ed\_in} \approx P_{ed\_out} \approx 0.5 P_{e\_midpl.}$) in both polarities at these main plasma parameters.

A cold but rather dense plasma ($T_{ed} = 2\text{–}8$ eV, $N_{ed} = 0.5\text{–}2 \times 10^{19}$ m^{-3}) accumulates in the private flux region, below the X point, and flows towards the outer divertor plate (which is the closer one in DIV-I geometry). The flow direction is reversed only near the inner separatrix leg.

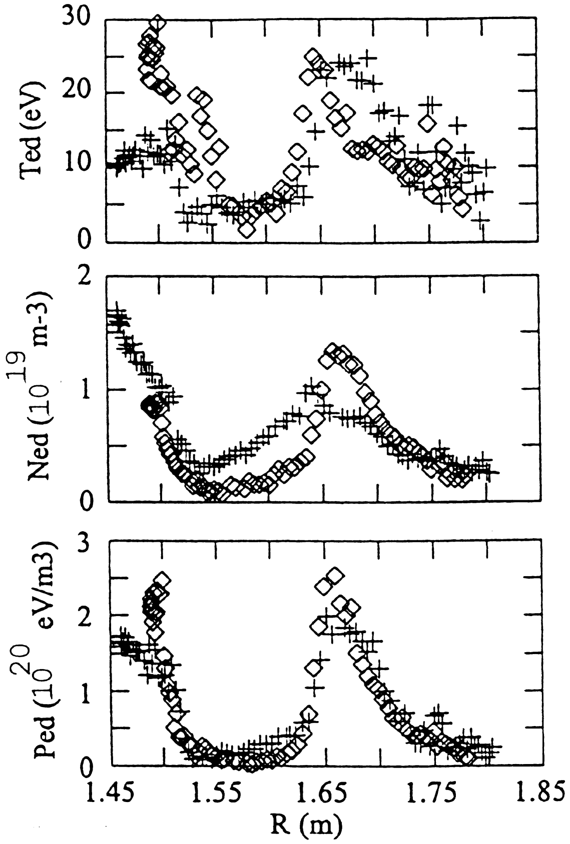

Fig. 2. Profiles in DIV-I geometry: (+) – normal polarity, (◇) – reverse polarity.

3.2. DIV-II profiles. The influence of divertor geometry

Stronger in/out asymmetries in the divertor plasma parameters have been recorded in the new DIV-II configuration (only normal polarity shots). While the profiles of plasma parameters in the outer divertor are similar to that of DIV-I, the inner leg profiles are strongly affected. This behaviour is evident in the evolution of divertor profiles during the main plasma density ramp towards the density limit (DL) in OH/DL shots ($I_p = 600$ kA, $B_t = -2$T) (Fig. 3). The electron temperature at the inner leg drops to low levels ($T_{ed\_in} < 10$ eV) even for low values of $\langle N_e \rangle$ and the density and particle flux profiles are peaked inward, 5–10 cm away from the separatrix. A pressure imbalance develops between the two divertors, announcing an early detachment of the inner leg.

On the way to DL the drop of electron temperature to less than 5 eV is accompanied by a flattening of the density and pressure profiles. At the MARFE onset

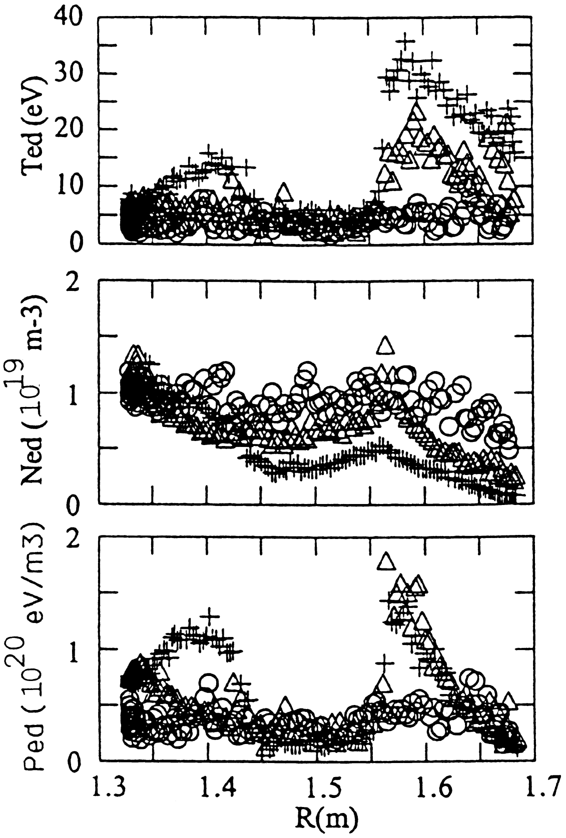

Fig. 3. Profiles in DIV-II geometry. (+) – $\langle N_e \rangle = 2 \times 10^{19}$ m^{-3}, (△) – $\langle N_e \rangle = 3 \times 10^{19}$ m^{-3}, (○) – $\langle N_e \rangle = 4.5 \times 10^{19}$ m^{-3}.

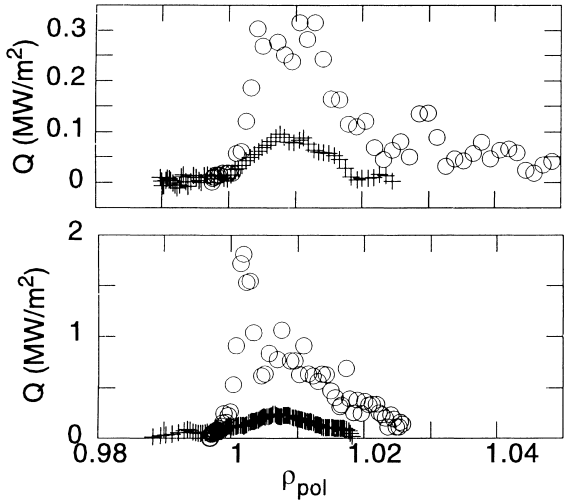

Fig. 4. Power flux profiles. (○) – Langmuir probes, (+) – thermography.

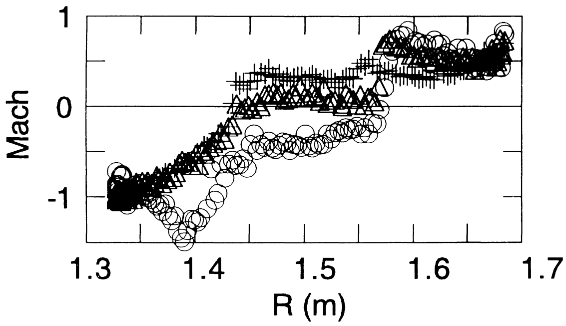

Fig. 5. Plasma flow profiles. (+) – $\langle N_e \rangle = 2 \times 10^{19}$ m^{-3}, (△) – $\langle N_e \rangle = 3 \times 10^{19}$ m^{-3}, (○) – $\langle N_e \rangle = 4.5 \times 10^{19}$ m^{-3}.

(which is the typical end for these OH/DL shots) T_{ed} and, mainly, N_{ed} drop further strongly.

3.3. Power flow into the divertor

The power flux to the probe, calculated at floating potential [7], has been compared with that recorded by thermography at the divertor targets. For DIV-I shots (Fig. 4(a)) a scaling factor of ≈ 3 is necessary to match the LPS profiles with the thermography, similar to that estimated from the mid plane probe/thermography comparison [8]. For the DIV-II geometry and OH shots, the power to the outer divertor leg at the LPS position is similar to that of DIV-I configuration, but the one reaching the divertor plates is too low to allow any estimation. During the few low power NI heated shots (2 MW NI) for which we get data the scaling factor was above 10 (Fig. 4(b)).

3.4. Plasma flow patterns

Complex flow patterns have been revealed by the 'Mach probe' during OH and NI shots (Fig. 5). In the connected part of the profiles the plasma flow is towards the divertor plates, at $M \leqslant 0.5$. Higher Mach numbers ($M = 0.8$–1) are observed at the inner divertor leg. These observations are in agreement with the data from spectroscopic measurements [9]. In the attached cases the flow changes direction at the inner separatrix, while the cold plasma below the X point, in the private flux region, flows towards the outer divertor plate. When the inner divertor evolves to detachment, the flow reversal position is shifted outwards till the outer separatrix is reached. In the accuracy of separatrix positioning we cannot decide if the flow reversal point accesses the connected region of the outer divertor leg.

The floating potential profiles (Fig. 6) are very similar to those observed in ASDEX [10], JET [11] and DIII-D [12]. They reveal complex current structures flowing into the divertor, depending on **B** direction, and allow an alternative localisation of the separatrix position with a good accuracy [3,10].

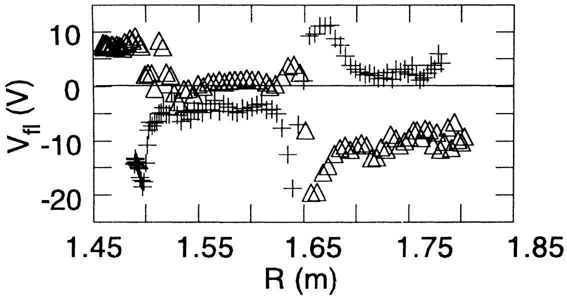

Fig. 6. Floating potential profiles, (△) – normal polarity, (+) – reverse polarity.

4. Discussion and conclusions

Some of the results presented above (profile and power flow sensitivity on ion grad**B** direction, floating potential profiles and currents in the SOL, etc.) are similar to that observed in other tokamaks. [1–3,10–12]. The number and the complexity of mechanisms able to produce such effects [13–15] and the implication for a specific machine, still requires a dedicated investigation and modelling effort for detailed understanding.

The power flux reaching the divertor targets proves to be sensitive to divertor geometry. Our results imply that strong losses and dispersion mechanisms occur in the two divertor legs, *bellow the LPS trajectory level*. These results are confirmed by recent bolometric and spectroscopic measurements [16] and supported by B2-Eirene code calculations [17]. Understanding and, eventually, influencing the plasma flow in the divertor region are very important for the successful operation of divertors. To study such flows Mach probe arrangements have been used in many tokamaks. To our knowledge, no completely acceptable theory for the Mach probe interpretation, especially for the connected SOL, is available. Even the smallest possible Mach probe arrangement creates its own 3D SOL. The data presented above have been processed using the fluid model results of Hutchinson [18] and Chung [19]. A modelling effort has also started using B2 code in the specific geometry of ASDEX-Upgrade. Despite the inherent uncertainties in absolute M evaluation, some of our results are reproduced surprisingly well by the B2 Eirene calculations [17].

References

[1] G.F. Matthews, Plasma Phys. Control. Fusion 36 (1994) 1595.
[2] B. LaBombard et al., J. Nucl. Mater. 241–243 (1997) 149.
[3] J.G. Watkins et al., J. Nucl. Mater. 241–243 (1997) 645.
[4] K. Guenther, 22nd EPS Conf. Control. Fusion and Plasma Physics, Bournemouth, 1995, p. I-433.
[5] EURATOM ERB 5000 CT 91007 Contract.
[6] N. Tsois et al., Demo-Report-98, to be published.
[7] P.C. Stangeby, Phys. Fluids 27 (1984) 3.
[8] V. Rhode et al., 23rd EPS Conf. Control. Fusion and Plasma Physics, Kiev, 1996, 811.
[9] J. Gafert et al, Plasma Phys. Control. Fusion 39 (1997) 1981.
[10] N. Tsois et al., 14th EPS Conf. Control. Fusion and Plasma Physics, Madrid, 1987, p. II-658.
[11] P.J. Harbour et al., J. Nucl. Mater. 162–164 (1989) 236.
[12] D. Buchenaur et al., J. Nucl. Mater. 176/177 (1990) 528.
[13] R. Chodura, 17th EPS Conf. Control. Fusion and Plasma Physics, Amsterdam, 1990, p. III-1443.
[14] F.L. Hinton, Y.-B. Kim, Nucl. Fusion 34 (1994) 899.
[15] A.V. Chankin, J. Nucl. Mater. 241–243 (1997) 199.
[16] A. Herrmann et al., these Proceedings.
[17] R. Schneider and the ASDEX Upgrade team, these Proceedings.
[18] I.H. Hutchinson, Phys. Fluids 30 (1987) 3777.
[19] K.-S. Chung, Phys. Plasmas 1 (1994) 2864.